Food Chemistry: X 27 (2025) 102365

Contents lists available at ScienceDirect

Food Chemistry: X

journal homepage: www.sciencedirect.com/journal/food-chemistry-x

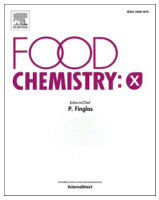

Metal ions binding and colloidal destabilization in the model systems: Implication on the magnesium chloride coagulation mechanism in tofu making

Qianru Li [a,b], Yufei Hua [a,b,*], Xingfei Li [a,b], Xiangzhen Kong [a,b], Caimeng Zhang [a,b], Yeming Chen [a,b]

[a] State Key Laboratory of Food Science and Resources, Jiangnan University, Wuxi, PR China
[b] School of Food Science and Technology, Jiangnan University, Wuxi, PR China

ARTICLE INFO

Keywords:
Tofu
Magnesium coagulation
Isothermal titration calorimetry
Metal ion binding
Colloidal particles
Zeta potential

ABSTRACT

$MgCl_2$-induced soymilk coagulation mechanism in tofu making was explored from perspectives of Mg^{2+} binding and colloidal properties in model systems. Isothermal titration calorimetry of bovine serum albumin (BSA)-small molecule mixtures revealed proteins contributed negligibly to Mg^{2+} binding sites, instead, substantial Mg^{2+} were bound by soymilk-borne small molecules. The results thus suggested the "protein-Mg^{2+}-protein bridge" was hardly formed in tofu making. Zeta potentials for both BSA-small molecule system and defatted soymilk changed in a similar pattern relative to the unbound Mg^{2+} concentration, indicating only those small molecules-unbound Mg^{2+} effectively neutralized the electronegative charges on protein colloidal particles. Turbidity and particle size results revealed a critical zeta potential (−11 mV) was required to induce marked Mg^{2+}-defatted soymilk coagulation. For heated defatted soymilks, a critical minimum protein concentration (8 mg/mL) was needed to observe the significant Mg^{2+}-induced coagulation. This study is expected to deepen our understanding of Mg^{2+} coagulation mechanism in tofu making.

1. Introduction

Magnesium chloride ($MgCl_2$), as a salt coagulant, is widely used to coagulate soymilk in tofu making. Currently, different theories have been proposed to explain the mechanism of $MgCl_2$-induced coagulation of soymilk. One of them is the cation bridge theory, which proposed that soy protein molecules are interacted with each other through the "protein-Mg^{2+}-protein bridge" to form gels. To form the "bridges", the divalent metal ions have to bind to the negatively charged groups on the different soy protein molecules, which accelerate the protein gelation rate and stabilize the formed three-dimensional gel network (Kao et al., 2003; Lee & Rha, 1978). Guan et al. (2021) proposed the salting-out mechanism to elucidate salt coagulation of soymilks in which the dehydration of the heat denatured soy proteins after the addition of salts played important role. However, protein salting-out is usually a reversible process, which is obviously contrary to the experimental phenomenon in the salt-induced soymilk coagulation that cannot be dissolved again. Another proposed salt coagulation mechanism suggested that the salt-induced reduction of pH and decrease in electrostatic repulsion between proteins promoted the aggregation of proteins (Wang, Wang, et al., 2023). Each explanation for the mechanism of salt coagulated soymilk has its own rationality and limitations, which needs further investigation.

Studies on the divalent metal ions (Mg^{2+} or Ca^{2+}) binding to soy proteins or soymilks have been reported by several authors. Saio et al. (1967) speculated that the binding sites for the divalent metal ions were those free carboxyl groups on the proteins. Rao and Rao (1975) reported that the divalent metal ions appeared to bind to the imidazole groups of histidine residues on the 7S proteins at pH 7.8 but no binding at pH 5.5. Sakakibara and Noguchi (1977) determined that 4–11 mol Ca^{2+} was bound to 10^5 g of 11S proteins at pH 8.0 but the binding was negligible at pH 6.0 and 7.0.

Phytic acid in the soymilk was reported to bind the divalent metal ions in the salt-induced soymilk coagulation process (Kumagai et al., 2002; Saio et al., 1967). Isothermal titration calorimetry (ITC) is a powerful technique used to explore the divalent metal cation-ligand

* Corresponding author at: State Key Laboratory of Food Science and Resources, Jiangnan University, 1800 Lihu Avenue, Wuxi 214122, Jiangsu Province, PR China.
E-mail address: yfhua@jiangnan.edu.cn (Y. Hua).

https://doi.org/10.1016/j.fochx.2025.102365
Received 9 September 2024; Received in revised form 14 February 2025; Accepted 9 March 2025
Available online 13 March 2025

interaction and provide the precise thermodynamic parameters of the interaction process (Johnson et al., 2016; Saponaro, 2018). Using ITC method, Canabady-Rochelle et al. (2009) found that the bound Ca^{2+} on the soy proteins decreased by 96.15 % after hydrolysis of proteins.

The coagulation of animal milks has been studied from the perspective of colloidal destabilization although this concept has been seldomly used in the study of soymilk coagulation (Horne & Banks, 2004). The casein micelle system is an excellent example of colloidal dispersion, of which the stability can be explained using the DLVO (Derjaguin-Lamdau-Verwey-Overbeek) theory and the presence of a sterically stabilizing effect (Horne & Banks, 2004; Narong & James, 2006).

Zeta potential is an important parameter and the absolute value of zeta potential characterizes the strength of the repulsive force between particles (Serrano-Lotina et al., 2023). Philippe et al. (2005) reported that the addition of 8.0 mmol/kg calcium and magnesium reduced zeta potential by −2.8 and − 3.5 mV, respectively. The decreases in zeta potential were proposed to be caused by neutralization of electronegative charges, the re-distribution of charged groups at the micellar surface and the changes in the overall thickness of the steric layer. Bauland et al. (2020) found that $MgCl_2$ or $CaCl_2$ additions reduced the zeta potential of casein micelles. Zhao et al. (2021) studied the effects of adding calcium chloride on the colloidal properties of the goat milk and their results showed that with the increase of $CaCl_2$ concentration, turbidity increased but the absolute value of zeta potential decreased.

Currently, neither the "protein-Mg^{2+}-protein bridge" nor the colloidal destabilization theory has shown sufficient evidence to support their validity in elucidating the Mg^{2+}-induced coagulation of soymilks. ITC, zeta potential, particle size and turbidity are well known methods of studying metal binding and colloidal properties. However, direct measurement of full fat soymilk was difficult to obtain desirable results due to the sample heterogeneity and the components cross interaction. Therefore, defatted soymilk based model systems were used and the purpose of this study was to provide more experimental evidences to deepen our understanding of the mechanism of $MgCl_2$-induced coagulation of soymilks.

2. Materials and methods

2.1. Materials

Freshly prepared low denatured defatted soybean meals were obtained from Shandong Yuwang Co., Ltd. and stored at 4 °C. Magnesium chloride hexahydrate was obtained from Sinopharm Chemical Reagent Co., Ltd. Bovine serum albumin (BSA) with purity of 98 % was purchased from Shanghai yuanye bio-technology Co., Ltd. Phytate solution (50 % (*w*/w)) was purchased from TCI Huacheng Industrial Development Co., Ltd. and other chemical reagents are of analytical grade.

2.2. Preparation and heat treatment of defatted soymilk

Defatted soybean meals were extracted by deionized water at a solid liquid ratio of 1:6 (w/w) and kept stirring at pH 7.0 and 25 °C for 1 h. After filtered through four layers of gauze, the filtrate was centrifuged (Himac CR21GII, Hitachi, Ltd., Shanghai, China) at 18,800*g* and 25 °C for 30 min to obtain the clarified supernatant, which was diluted with deionized water to the 40 mg/mL protein concentration (N*6.25) and specified as unheated defatted soymilk.

Ten milliliters of freshly prepared defatted soymilk (protein concentration adjusted to 40 mg/mL) was pipetted into the high boron silicate threaded heat-resistant tube and pre-heated at the predetermined temperature oil bath to the designated temperatures (65, 75, 85, 90, 95, 100, 105 and 115 °C) within 3 min, then incubated in another oil bath at the designated temperatures for 5 min followed by immediate cooling in ice bath to room temperature.

2.3. Determination of phytate content of the defatted soymilk

Phytate content in defatted soymilk was determined according to the method of Chen et al. (2022). Five milliliters of defatted soymilk was mixed with 15 mL of 2.4 % (*v*/v) HCl solution and stirred at room temperature for 2 h. The mixed solution was centrifuged at 2000*g* and 25 °C for 20 min (Himac CR21GII, Hitachi, Ltd., Shanghai, China) and the supernatant was added with 2 g of NaCl followed by sufficient stirring to completely dissolve the NaCl. After cooling in the ice bath, the mixture was centrifuged at 12,000*g* and 4 °C for 20 min. The supernatant was diluted with deionized water to a final volume of 50 mL in a volumetric flask and then 5 mL of this solution was taken out and mixed with 4 mL of Wade reagent (0.30 % sulfosalicylic acid +0.03 % $FeCl_3{\cdot}6H_2O$). After thorough mixing, the mixture was centrifuged at 2000*g* and 10 °C for 10 min. The absorbance of the defatted soymilk sample was determined by a spectrophotometer at 500 nm (UV-1200, Hottie company, Ltd., Shanghai, China). Standard curve was obtained by mixing 5 mL of sodium phytate solution with concentration between 0.0008 mg/mL and 0.1 mg/mL with 4 mL of Wade reagent and centrifuged under the same condition.

2.4. Determination of citrate content of the defatted soymilk

The content of citrate in the defatted soymilk was determined according to the method reported by Madjirebaye et al. (2022) and Zheng et al. (2021) with slight modifications. The defatted soymilk (1.5 mL) was mixed with 8 mL of 0.1 mol/L sulfuric acid solution and brought to the volume of 10 mL using distilled water. After centrifuging at 11,000 g and 25 °C for 30 min, the supernatant was filtered through a 0.22 μm organic membrane. HPLC (Agilent 1100, USA) analysis was conducted using the following conditions: chromatography column of diamonsil C18 (4.6 mm × 250 mm, 5 μm); flow rate of 0.8 mL/min; column temperature of 30 °C; injection volume of 5 μL; detection wavelength of 210 nm; mobile phase A of methanol / water / H_3PO_4 (5 / 95 / 0.05, *v*/v/v) and mobile phase B of methanol /water / H_3PO_4 (80 / 20 / 0.05, v/v/v).

2.5. Determination of total polyphenol content of the defatted soymilk

Total polyphenol content in the defatted soymilk was determined using the Folin-Ciocalteu reagent according to the method reported by Benherlal and Arumughan (2007) with slight modifications and expressed as gallic acid equivalent (GAE). The defatted soymilk was mixed with ethanol to the final ethanol concentration of 80 % and ultrasonically stirred at 40 °C for 60 min. After centrifugation at 10,000 *g* and 4 °C for 20 min, the supernatant was collected. Standard solution was obtained by diluting the stock solution of gallic acid with deionized water to the concentration range of 0–6 μg/mL. The ethanol extract and gallic acids standard solution were mixed with Folin-Ciocalteu reagent (0.1 mL/1.0 mL), respectively. After keeping at 25 °C for 5 min, 2 mL of 15 % aqueous sodium carbonate was added and brought to 10 mL using distilled water. After incubating at 25 °C for 60 min, the absorbance of the sample was measured at 760 nm against a reagent blank.

2.6. Preparation of soymilk borne polyphenol

Soymilk borne polyphenols were prepared by mixing defatted soymilk with ethanol to the final ethanol concentration of 80 % and ultrasonically treated at 40 °C for 60 min. Following centrifuging at 10,000 g and 4 °C for 20 min, the collected supernatant was concentrated at 60 °C under vacuum (0.01 MPa) to remove ethanol and then freeze-dried.

2.7. Isothermal titration calorimetry

A MicroCal PEAQ-ITC (Malvern company, U. K.) was used to perform

the ITC experiments and to obtain the thermodynamic characterization of the interactions. Titrations were carried out under constant stirring (750 rpm) at 25 °C. The sample cell was titrated by $MgCl_2$ solution with concentration of 5.49×10^{-3} mol/L. The first injection was 0.4 μL and followed by 18 injections of 2 μL, with 60 s intervals between each injection.

The dilution heat (injected $MgCl_2$ to deionized water in the same way) was subtracted from the sample data and the corrected binding data was fitted by "one-site" model of the instrument's built-in analysis software. Thermodynamic parameters, such as stoichiometry (n), binding constant (K_a), enthalpy change (ΔH), entropy change (ΔS) and binding Gibbs free energy (ΔG) were determined. Previous experiments found that when titrating Mg^{2+} into the same molar number of phytate, citric acid, and polyphenols, the heat release was similar. Therefore, to process the "one-site" model fitting of the mixed systems (phytate + citric acid, and phytate + citric acid + polyphenols), the molar numbers of different small molecules were added up and used as the molar concentration of sample cells.

2.8. Zeta potential

The zeta potential of samples was measured by electrophoretic light scattering using a dynamic light scattering analysis on a Zetasizer Nano ZEN3700 (Malvern company, U. K.) device at 25 °C and 173° scattering angle (Serrano-Lotina et al., 2023). Electrophoresis is the movement of charged colloidal particles in liquids under the effect of an external electric field. Defatted soymilks were diluted to the targeted protein concentration and coagulated by $MgCl_2$ at 25 °C for 30 min before measurement. The Henry equation was used to calculated the zeta potential as follows:

$$\text{zeta potential} = \frac{3U_E{}^*\eta}{2\varepsilon{}^*f(ka)} \quad (1)$$

U_E is the electrophoretic mobility ($m^2\ V^{-1}\ s^{-1}$), which is the electrophoretic velocity divided by the electric field strength and measured by the Zetasizer Nano ZEN3700 machine. η is the viscosity ($kg\ m^{-1}\ s^{-1}$) and ε is the solvent dielectric permittivity ($kg\ m\ V^{-2}\ s^{-2}$). The f(ka) is the Henry function (dimensionless) and the value applied in this study is 1.5 (Smoluchowski approximation) because of the polar medium of water.

2.9. Particle size measurement

The particle size of defatted soymilk was measured by dynamic light scattering based on the Brownian motion of particles that caused the dynamic fluctuations of light scattering intensity (Gołębiowski & Buszewski, 2023). The particle size was calculated via the Stokes-Einstein equation based on the Zetasizer Nano ZEN3700 (Malvern company, U. K.) machine measured diffusion coefficient that analyzed by the intensity fluctuations.

$$\text{Particle size} = \frac{k_B{}^*T}{6\pi{}^*\eta{}^*D} \quad (2)$$

where k_B is the Boltzmann constant, T is the absolute temperature, η is the sample viscosity and D is the diffusion coefficient. Defatted soymilks were diluted to the targeted protein concentration for measurement, and the defatted soymilks with $MgCl_2$ addition were incubated at 25 °C for 30 min before measurement. The particle size increment was defined as the particle size change of defatted soymilk before and after the Mg^{2+} addition.

2.10. Turbidity measurement

Determination of turbidity was performed on a spectrophotometer (UV-1200, Hottie Lab Co., Ltd., Shanghai, China) at 25 °C with a wavelength of 600 nm (Huang et al., 2024). The turbidity of defatted soymilks was determined at 25 °C. The previous experiment showed that after mixing defatted soymilks with $MgCl_2$ solution, turbidity increased progressively with time and became essentially stable at about 30 min. Therefore, turbidity was recorded after 30 min of defatted soymilk–$MgCl_2$ mixing. The turbidity increment was defined as the turbidity change of defatted soymilk before and after the Mg^{2+} addition.

2.11. Calculation of unbound Mg^{2+} concentration

The binding of Mg^{2+} ions can be expressed by the following equilibrium:

$$M + B \overset{K_a}{\rightleftharpoons} MB \quad (3)$$

where M, B, K_a and MB are the metal ion, binding site, binding constant and bound product, respectively.

The concentration of unbound Mg^{2+} is expressed as:

$$[M_U] = [M_T] - [MB] \quad (4)$$

$[M_U]$ is the concentration of unbound Mg^{2+}, $[M_T]$ is the total Mg^{2+} concentration that added to the system, $[MB]$ is the concentration of bound product.

In the case of $K_a \gg 1$, almost all binding sites were bound by Mg^{2+} to generate MB, so the concentrations of MB are almost equal to the concentrations of B:

$$[B] \approx [MB] \quad (5)$$

The concentration of binding sites can be calculated from the concentration of small molecules ($[M]$) and the binding site number (n) obtained from the model fitting of ITC data:

$$[B] = [M]^*n \quad (6)$$

Therefore, the concentration of unbound Mg^{2+} is calculated as follows:

$$[M_U] = [M_T] - [M]^*n \quad (7)$$

2.12. Statistical analysis

All data were obtained from three independent experiments and expressed as the mean ± standard deviation. Error bars presented in figures indicate standard deviations. Data analysis was performed using IBM SPSS 24.0 software and Tukey's multiple range test was selected with a significance level of 0.05.

3. Results and discussion

3.1. Thermodynamic properties of Mg^{2+} binding

3.1.1. Concentration of small molecules in the defatted soymilk

Concentrations of phytate, citrate and polyphenol of the defatted soymilk with protein concentration of 4.0 mg/mL were determined as 6.00×10^{-2}, 4.29×10^{-1} and 5.40×10^{-3} mg/mL, respectively. The molar concentrations of phytate, citric acid and polyphenol were calculated as 9.09×10^{-5}, 2.23×10^{-3} and 3.17×10^{-5} mol/L using the molar mass of 660.04, 192.13 and 170.12 g/mol, respectively.

3.1.2. ITC result from Mg^{2+} titration to the defatted soymilk

Fig. 1A shows the net ITC heat flow related to the titration of $MgCl_2$ into defatted soymilk, which was obtained by subtracting the exothermic dilution heat of Mg^{2+} into deionized water under the same conditions from the total heat of Mg^{2+} into defatted soymilk. The upper panel shows the heat flow caused by the injection procedure. However, it was unexpected that net endothermic peaks were observed which are generally related to the dissociation reactions rather than the binding reactions. Several studies reported the same phenomenon (Canabady-Rochelle et al., 2009; Liu et al., 2023). It is suggested that the apparent

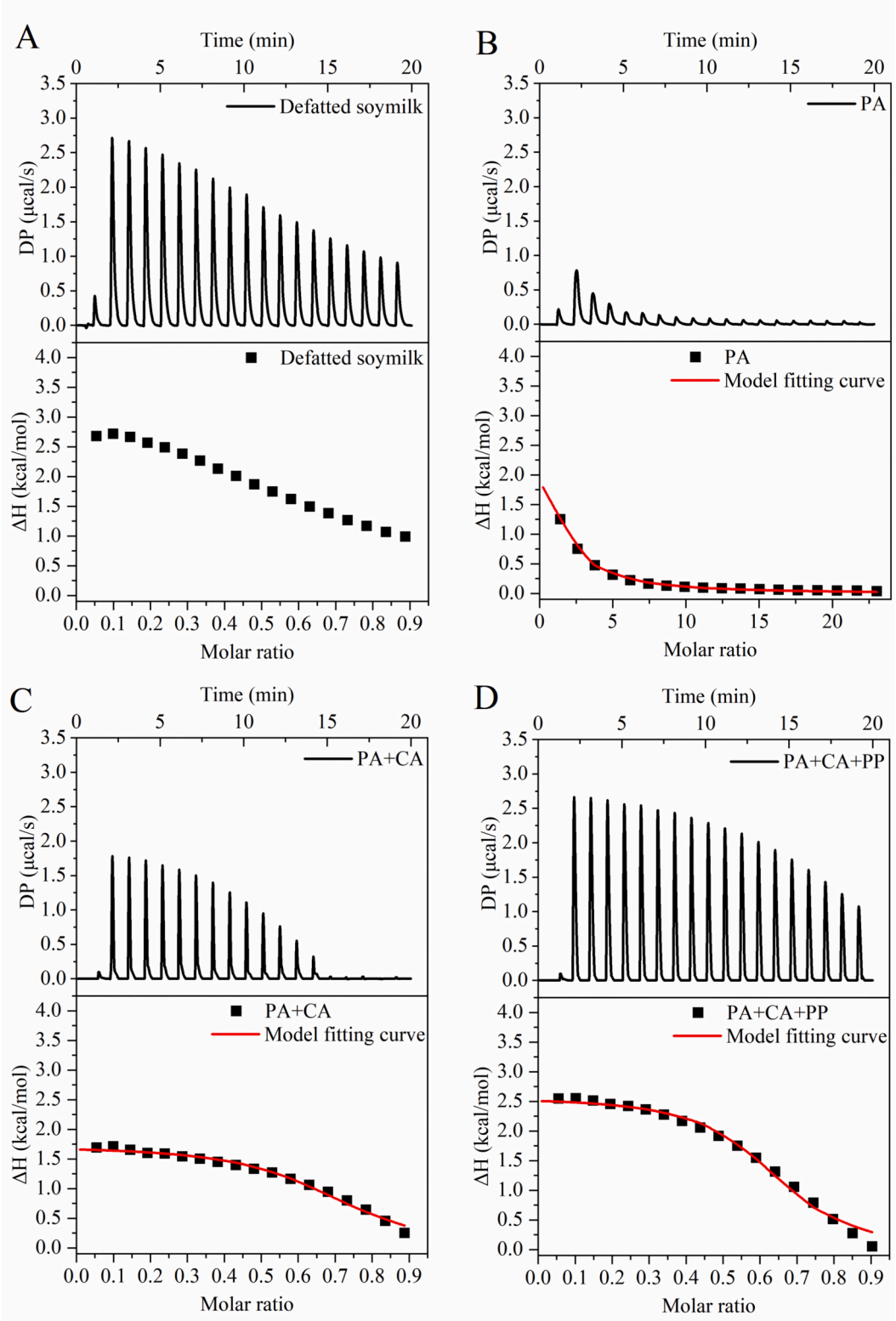

Fig. 1. Isothermal titration calorimetry data of titrating $MgCl_2$ into defatted soymilk (A) and small molecule solutions: PA (B), PA + CA (C), PA + CA + PP (D). PA, CA and PP refers to phytate, citrate and polyphenol.

endothermic effects were actually the combination of the relatively smaller exothermic effect related to the binding of Mg^{2+} to the ligands and the relatively larger endothermic effect due to the release of water molecules from the ligands.

3.1.3. *ITC result from Mg^{2+} titration to small molecules*

Solutions of phytate (PA), phytate and citrate (PA + CA) as well as phytate, citrate and polyphenol (PA + CA + PP) were prepared. The molar concentrations of PA, CA and PP in the above solutions were the same as those of the defatted soymilk (9.09×10^{-5}, 2.23×10^{-3} and 3.17×10^{-5} mol/L, respectively).

PA, PA + CA and PA + CA + PP were titrated by $MgCl_2$ solution and the results are shown in Fig. 1B, C and D. Endothermic peaks were also observed after correcting the $MgCl_2$ dilution heat from the raw data.

Results of one-site model fitting are shown in Table 1. The number of binding sites for Mg^{2+} to PA, PA + CA and PA + CA + PP were 0.357 mol/mol, 0.642 mol/mol and 0.702 mol/mol, respectively. At the same time, the binding constants (K_a) for PA + CA and PA + CA + PP were much higher than that for PA, suggesting that the binding affinity between Mg^{2+} and phytate + citrate as well as phytate + citrate + polyphenol was much higher than that between Mg^{2+} and phytate. Currently, it is not sure whether these small molecules act independently, synergistically or antagonistically. Some other studies reported the similar binding site number for Mg^{2+}-phytate system (Kim et al., 2010; Oh et al., 2007) but no report on the binding sites for Mg^{2+}-citrate and Mg^{2+}-polyphenol systems.

3.1.4. ITC result from Mg^{2+} titration to BSA-small molecule mixtures

To know whether or not proteins contributed the Mg^{2+} binding properties of the protein-small molecule mixtures, the defatted soymilk free from small molecule was the best choice. However, it was difficult to remove small molecules from the defatted soymilks without other uncontrollable effects, such as the growth of microbial during dialysis, the surface adsorption of proteins on the membrane, the incomplete removal of small molecules and other negative effects due to the complicated sample preparation steps. BSA is a pure protein with similar electrostatic properties (pI 4.7) to that of soy proteins (Kunde & Wairkar, 2022; Yıldız et al., 2020). Therefore, BSA was used in the present study in case of investigating the protein-small molecules cross interactions in ITC and zeta potential analysis.

ITC experiments was conducted by titrating $MgCl_2$ into BSA solution and BSA–small molecules mixtures, in which the concentrations of small molecules were the same as those in the above section. Fig. 2A shows the ITC data generated by titrating $MgCl_2$ into BSA solution. After correcting the $MgCl_2$ dilution heat from the raw data, only very small net heat was obtained and failed to be fitted by one-site model. Kaspchak et al. (2018) also found that $MgCl_2$ titration into BSA solution only resulted in small positive enthalpy changes and no fitting result could be obtained. Therefore, our experiment indicated that no direct binding of Mg^{2+} to the protein molecules.

Fig. 2B, C and D show the net endothermic peaks of titrating $MgCl_2$ into BSA–small molecules mixtures after correcting the $MgCl_2$ dilution heat from the raw data, which gave peak amplitudes very similar to those in Fig. 1B, C and D, respectively. One-site model fitting was conducted using the molar concentrations of small molecules and the sum of the molar concentrations of small molecules and BSA as the cell concentration and the results are shown in Table 2. Obviously, model fitting of the protein containing small molecule system yielded binding parameters similar to those of protein free small molecule system when protein concentration was not involved. However, when molar concentration of amino acid residues in BSA was considered in model fitting, much smaller binding parameters were obtained (Table 2), indicating that proteins did not contribute but "diluted" the Mg^{2+} binding ability.

Comparing Fig. 1A with Fig. 2D, a remarkable similarity was noticed. Since the concentrations of proteins and small molecules in both defatted soymilk and BSA system were the same, it was reasonable to propose that the Mg^{2+} binding in defatted soymilks was also contributed mostly by small molecules.

Table 1
Thermodynamic parameters of $MgCl_2$ binding to small molecule solutions.

Samples	Model fitting parameters				
	N (sites, mol/mol)	K_a (L/mol)	ΔH (kcal/mol)	ΔG (kcal/mol)	-TΔS (kcal/mol)
PA	0.357 ± 0.007^{c}	3976.19 ± 11.22^{c}	8.61 ± 0.29^{a}	−4.91 ± 0.00^{a}	−13.50 ± 0.28^{c}
PA + CA	0.642 ± 0.019^{b}	23,626.39 ± 1634.42^{a}	1.28 ± 0.01^{b}	−5.97 ± 0.04^{b}	−7.26 ± 0.04^{b}
PA + CA + PP	0.702 ± 0.007^{a}	16,478.09 ± 345.52^{b}	0.87 ± 0.02^{c}	−5.76 ± 0.01^{c}	−6.63 ± 0.02^{a}

PA, CA and PP refers to phytate, citrate and polyphenol.
Different letters in the same column indicate significant differences ($P < 0.05$).

3.2. Zeta potential and $MgCl_2$ coagulation

3.2.1. Zeta potential of $MgCl_2$ coagulated systems

Zeta potential is a useful parameter to characterize the surface potential of colloid particles, which signifies the particle's stability (Patra et al., 2021). Zeta potentials of $MgCl_2$ coagulated BSA solution and defatted soymilks are shown in Fig. 3.

Fig. 3A shows the zeta potentials for BSA, BSA + PA, BSA + PA + CA and BSA + PA + CA + PP when different levels of $MgCl_2$ were added. Before adding $MgCl_2$, both BSA and BSA–small molecule mixtures presented the zeta potential values around −26 mV, indicating that zeta potentials of colloidal particles were not affected by the presence of small molecules. Otherwise, more negative zeta potential values were found for BSA–small molecule mixtures due to the combining of negative charged small molecules to protein colloidal particles. With the increase of $MgCl_2$ levels, absolute values of zeta potential decreased, signifying the neutralization of electronegativity on the colloidal particles. However, the extent of neutralization diminished as more small molecules were introduced into the systems.

From Fig. 3B, it is learned that the absolute values of zeta potential for Mg^{2+} coagulated unheated and heated defatted soymilks were almost the same, indicating that the heat denaturation of proteins did not affect the neutralization of electronegativity on the colloidal particles. The data shows that the absolute zeta potential values decreased rapidly when the $MgCl_2$ concentration was below 3.0 mmol/L but became less steep for higher $MgCl_2$ concentrations.

In Fig. 3C, the absolute value of zeta potentials for both Mg^{2+} coagulated unheated and heated defatted soymilks increased with the rising of protein concentration in almost the same way, indicating that, with the elevation of protein/$MgCl_2$ ratio, less electronegativity on the colloidal particles was neutralized.

Fig. 3D shows the effect of phytate concentration on the colloidal properties of Mg^{2+} coagulated defatted soymilks. For phytate contents lower than 2 times that of the defatted soymilk, more electronegativity was neutralized by Mg^{2+} and lower zeta potential absolute values were obtained. With the increase of phytate content, the neutralization effect was suppressed and higher zeta potential absolute values were found.

The above experiments showed that zeta potential of defatted soymilk and BSA-small molecule system was affected by many factors. Several studies found that increasing Mg^{2+} or Ca^{2+} concentrations lead to a decrease in the absolute value of zeta potential (Kulmyrzaev et al., 2000; Wang et al., 2015; Wang, Tan, et al., 2023). Wang et al. (2015) also reported the negative effect of phytate content on the reduction of the absolute value of zeta potential. However, there is a lack of the deep understanding of the behavior.

3.2.2. Effective $MgCl_2$ concentration as important factor determining zeta potential

The ITC experiments suggested that significant binding of Mg^{2+} by small molecules occurred in BSA-small molecules system and the binding is most probably also occurred in defatted soymilk. Therefore, unbound Mg^{2+} concentrations were calculated and the results are shown in Fig. 4.

Fig. 4A shows that the unbound Mg^{2+} concentrations for small molecule free BSA were the same as the added Mg^{2+} since no binding occurred. The unbound Mg^{2+} concentrations for BSA-small molecule mixtures were affected by composition of small molecules and the levels of added Mg^{2+}. At the 2 mmol/L Mg^{2+} addition level, the unbound Mg^{2+}

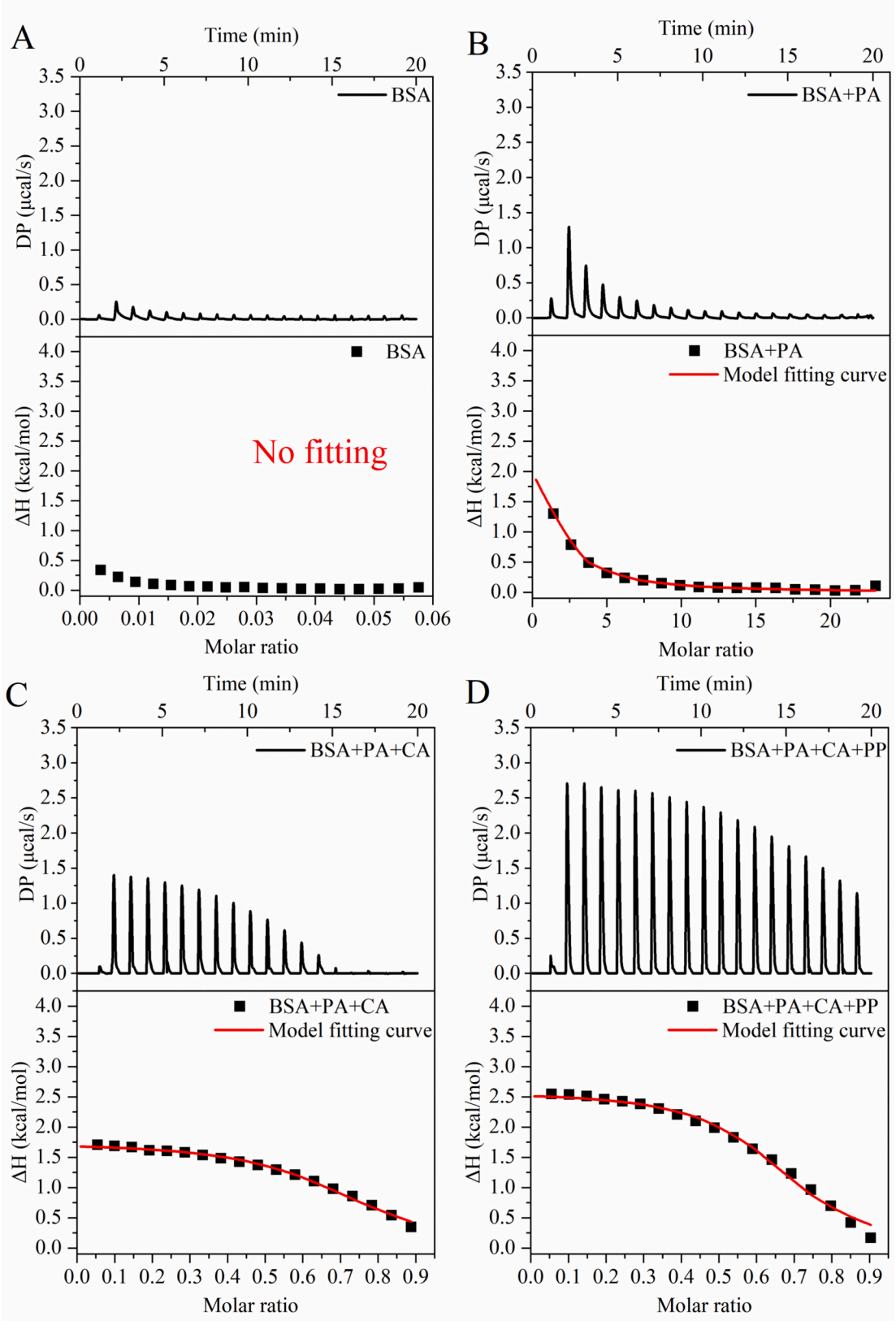

Fig. 2. Isothermal titration calorimetry data of titrating $MgCl_2$ into BSA (A) and BSA–small molecules mixtures: BSA + PA (B), BSA + PA + CA (C), BSA + PA + CA + PP (D). PA, CA and PP refers to phytate, citrate and polyphenol.

Table 2
Thermodynamic parameters of $MgCl_2$ binding to BSA – small molecules mixtures.

Samples	The molar concentrations of small molecules were used as the cell concentration					The sum of the molar concentrations of small molecules and BSA were used as the cell concentration				
	N (sites, mol/mol)	K_a (L/mol)	ΔH (kcal/mol)	ΔG (kcal/mol)	-TΔS (kcal/mol)	N (sites, mol/mol)	K_a (L/mol)	ΔH (kcal/mol)	ΔG (kcal/mol)	-TΔS (kcal/mol)
BSA + PA	0.362 ± 0.014^c	3984.13 ± 22.45^c	8.40 ± 0.58^a	−4.92 ± 0.01^a	−13.30 ± 0.57^c	0.001 ± 0.000^c	3978.84 ± 18.33^c	8.54 ± 0.47^a	−4.91 ± 0.01^a	−13.43 ± 0.46^b
BSA + PA + CA	0.648 ± 0.023^b	23,154.58 ± 2001.74^a	1.29 ± 0.01^b	−5.96 ± 0.05^b	−7.25 ± 0.05^b	0.039 ± 0.001^b	23,626.39 ± 1634.42^a	1.28 ± 0.01^b	−5.97 ± 0.04^b	−7.26 ± 0.04^a
BSA + PA + CA + PP	0.711 ± 0.017^a	15,887.35 ± 1051.95^b	0.87 ± 0.01^c	−5.73 ± 0.04^c	−6.60 ± 0.04^a	0.044 ± 0.001^a	15,887.35 ± 1051.95^b	0.87 ± 0.01^c	−5.73 ± 0.04^c	−6.60 ± 0.04^a

PA, CA and PP refers to phytate, citrate and polyphenol.
Different letters in the same column indicate significant differences ($P < 0.05$).

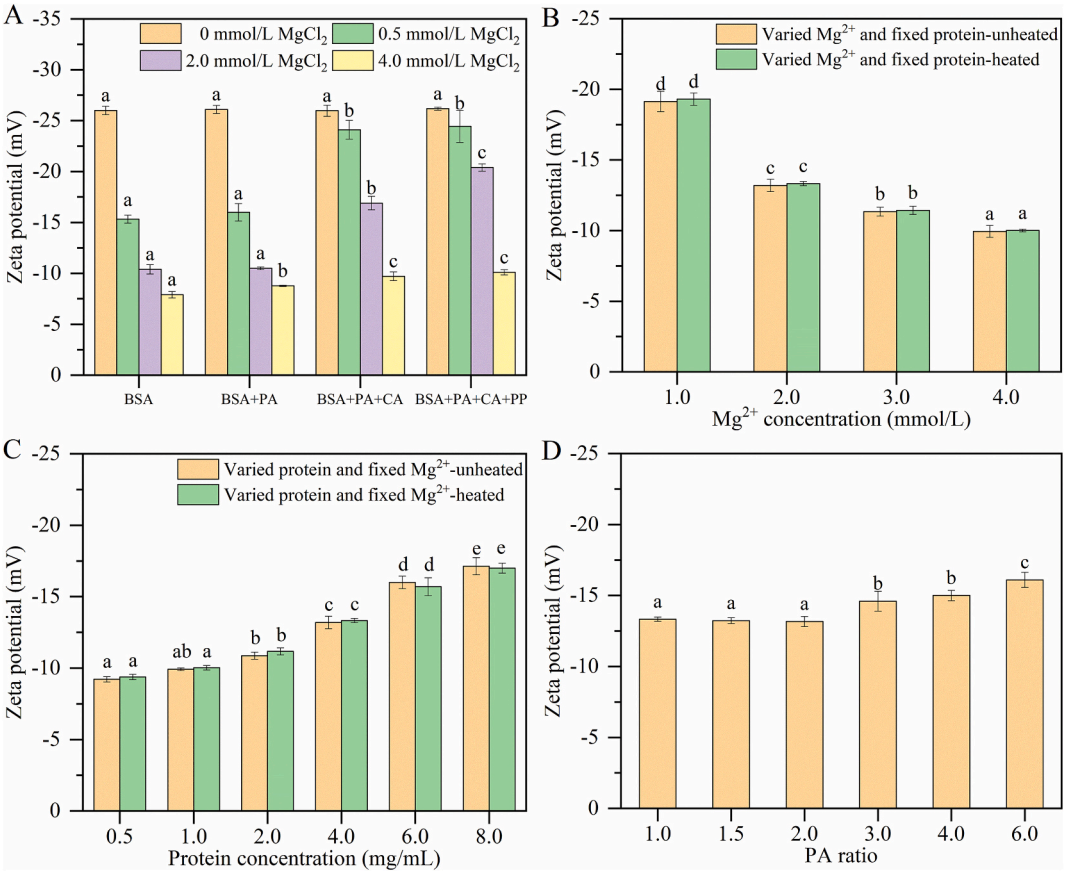

Fig. 3. Zeta potential of BSA–small molecule mixtures (BSA, PA, PA + CA and PA + CA + PP) coagulated with different concentrations of $MgCl_2$ (A), and of Mg^{2+} coagulated defatted soymilk with different Mg^{2+} concentration (B), different protein concentration (C) and different PA concentration (D). PA, CA and PP refers to phytate, citrate and polyphenol. Different letters in the same series indicate significant differences ($P < 0.05$).

accounted for 98.35 %, 24.65 % and 16.20 % of the added Mg^{2+} when the substrates were BSA + PA, BSA + PA + CA and BSA + PA + CA + PP, respectively.

Fig. 4B shows the unbound Mg^{2+} concentrations for defatted soymilk with the constant protein concentration of 4 mg/mL. At the Mg^{2+} addition level of 1.0 mmol/L, the calculated unbound Mg^{2+} concentration was nearly zero but it was about 2.3 mmol/L for Mg^{2+} addition level of 4.0 mmol/L.

From Fig. 4C, it is learned that the unbound Mg^{2+} concentrations for defatted soymilk with varying protein concentration and constant Mg^{2+} addition level of 2.0 mmol/L were nearly zero for protein concentrations of 6.0 and 8.0 mg/mL, respectively.

Fig. 4D shows the unbound Mg^{2+} concentrations for defatted soymilk as affected by phytate contents with the constant protein concentration and Mg^{2+} addition level of 4 mg/mL and 2.0 mmol/L, respectively. With the increase of phytate content, a monotonically decreased trend of unbound Mg^{2+} concentration was noticed.

In Fig. 4E, zeta potentials are plotted against the concentrations of unbound Mg^{2+} for BSA–small molecule mixtures and defatted soymilks and also against the concentration of added Mg^{2+} for small molecule free BSA. Surprisingly, it was found that, although the samples were different vastly, zeta potentials changed quite similarly with the increase of the concentrations of unbound or added Mg^{2+}.

Therefore, only unbound Mg^{2+} was effective in neutralizing electronegative charges on colloidal particles and thus reducing the absolute values of zeta potential. The rule held true for both BSA and defatted

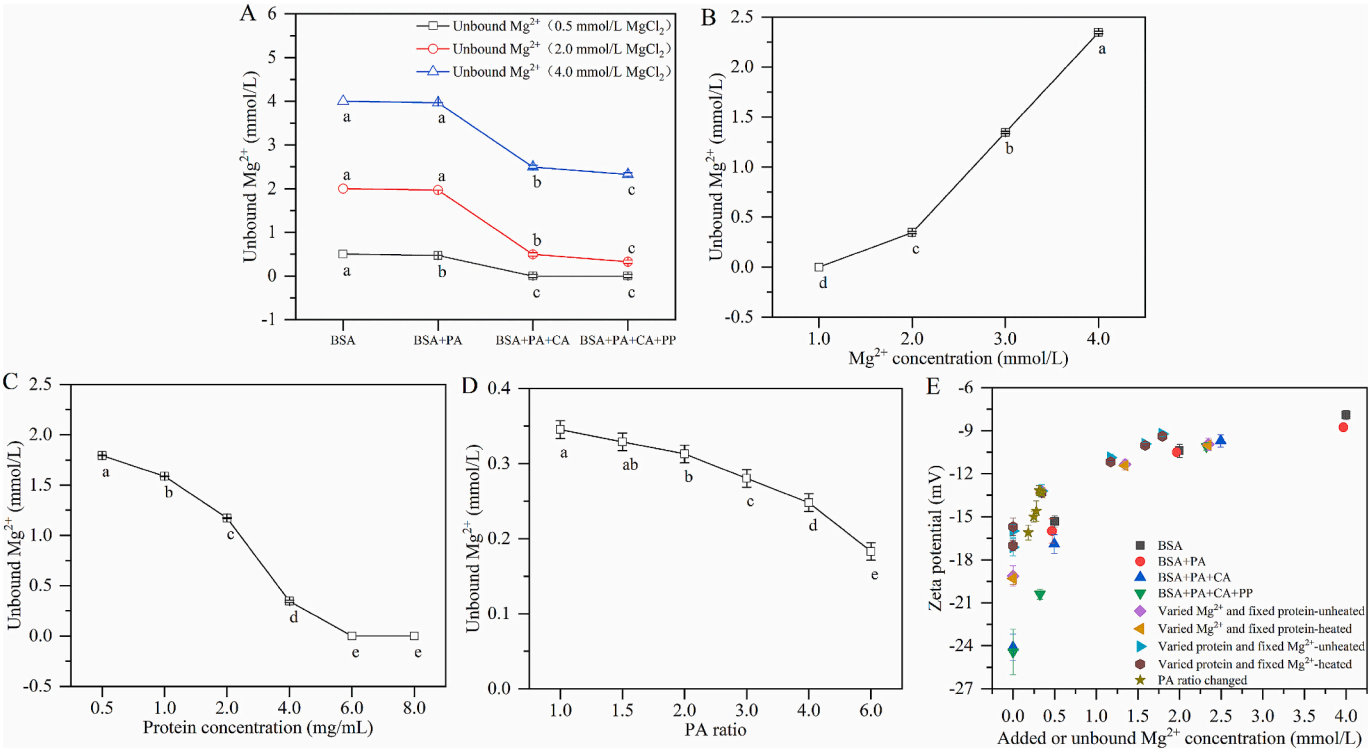

Fig. 4. Unbound Mg^{2+} for BSA–small molecule mixtures (BSA, PA, PA + CA and PA + CA + PP) coagulated with different concentrations of $MgCl_2$ (A), and for Mg^{2+} coagulated defatted soymilk with different Mg^{2+} concentration (B), different protein concentration (C), different PA concentration (D). Zeta potential at different added or unbound Mg^{2+} concentration (E). PA, CA and PP refers to phytate, citrate and polyphenol. Different letters in the same series indicate significant differences ($P < 0.05$).

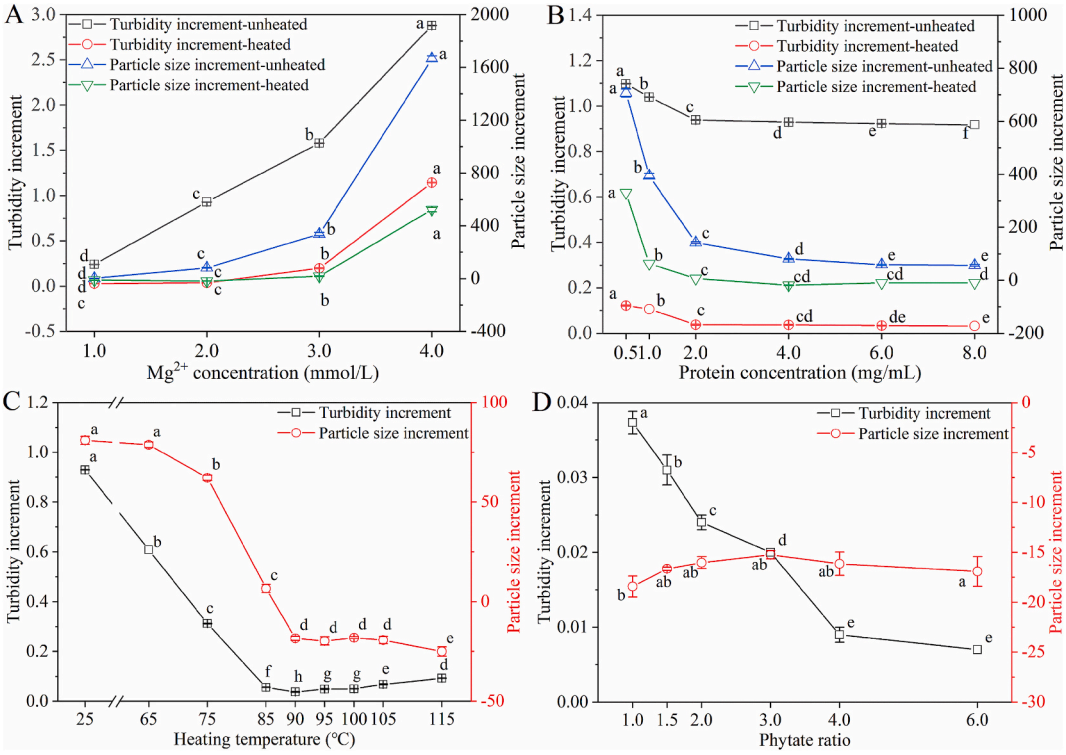

Fig. 5. Turbidity increment and particle size increment of Mg^{2+} coagulated defatted soymilk with different Mg^{2+} concentration (A), different protein concentration (B), different temperature heated defatted soymilk (C) and different PA concentration (D). Different letters in the same series indicate significant differences ($P < 0.05$).

soymilks. Obviously, more effective Mg^{2+} are available when the concentrations of small molecules are lower, and lower dosage of $MgCl_2$ is needed to reduce the zeta potential. This finding is important for improving tofu quality. By removing Mg^{2+} binding small molecules through soybean variety breeding or soymilk processing, tofu with less bitterness and a smoother texture is expected to be obtained.

3.3. Turbidities and particle sizes of the $MgCl_2$ coagulated defatted soymilks

3.3.1. Turbidities and particle sizes as affected by different parameters

To eliminate the sample background noise and focus on the effect of $MgCl_2$ coagulation, only increments of turbidity and particle size were discussed in Fig. 5.

Fig. 5A shows that turbidity increment of Mg^{2+} coagulated unheated defatted soymilk increased steadily with the increase of $MgCl_2$ concentration up to 3.0 mmol/L followed by a higher increasing trend at higher $MgCl_2$ concentrations. The turbidity increment of Mg^{2+} coagulated heated defatted soymilk was much lower than that of unheated defatted soymilk. The Figure also shows that the particle size increment of Mg^{2+} coagulated unheated and heated defatted soymilks did not change markedly for $MgCl_2$ concentration lower than 3.0 mmol/L. Zhao et al. (2021) found that there was no detectable change in the particle size of casein micelles of goat milk for $CaCl_2$ concentration lower than 5.4 mmol/kg. However, the particle size increment of Mg^{2+} coagulated unheated defatted soymilk increased rapidly for $MgCl_2$ concentration higher than 3.0 mmol/L. On the other hand, the particle size increment of Mg^{2+} coagulated heated defatted soymilk only increased moderately.

Defatted soymilks with increasing protein concentrations were coagulated by $MgCl_2$ solution at constant addition level of 2 mmol/L. Fig. 5B shows the vast difference in turbidity increment between the Mg^{2+} coagulated unheated and heated defatted soymilks. At the same time, a break point occurred around 2.0 mg/mL protein concentration were noticed for turbidity increments of both heated and unheated defatted soymilks. Fig. 5B also shows that a relatively sharp decreases in particle size increments of both Mg^{2+} coagulated unheated and heated defatted soymilks were observed when the protein concentration increased from 0.5 mg/mL to 2 mg/mL.

From Fig. 5C, it is known that both turbidity increment and particle size increment of the Mg^{2+} coagulated defatted soymilks decreased sharply with the increase of heating temperature and reached the minimum at 90 °C followed by gentle turbidity increment rise with further increase in heating temperature. The decreases of turbidity increment and particle size increment upon adding $MgCl_2$ to the heated defatted soymilks was probably related to the heat induced unfolding and the subsequent aggregation of soy proteins (Liang et al., 2020). When the positively charged Mg^{2+} was added, the neutralization of electronegative charges on the unfold protein molecules and aggregates resulted in the shrink of the proteins colloids. Besides, larger particle sized protein aggregates in heated defatted soymilk displayed higher hydrodynamic drags. As a consequence, the Mg^{2+} coagulation induced combine became more difficult as compared with proteins in unheated defatted soymilks.

Fig. 5D reveals that turbidity increment decreased slightly but particle size increment remained almost unchanged even though the content of phytate had been increased 6-fold. In other words, the content of phytate had little effect on the Mg^{2+} coagulation of defatted soymilk.

3.3.2. Critical zeta potential and critical protein concentration

The above section revealed that zeta potential, turbidity and particle size changed in different ways as the operational parameters ($MgCl_2$ concentration, protein concentration and heating temperature) and phytate content were modulated. To further disclose the colloidal properties of the Mg^{2+} coagulated defatted soymilks, increments in the turbidity and particle size as a function of zeta potential were investigated and the results are displayed in Fig. 6.

Fig. 6A shows the dependences of turbidity increment and particle size increment on the zeta potential in the case of fixed protein

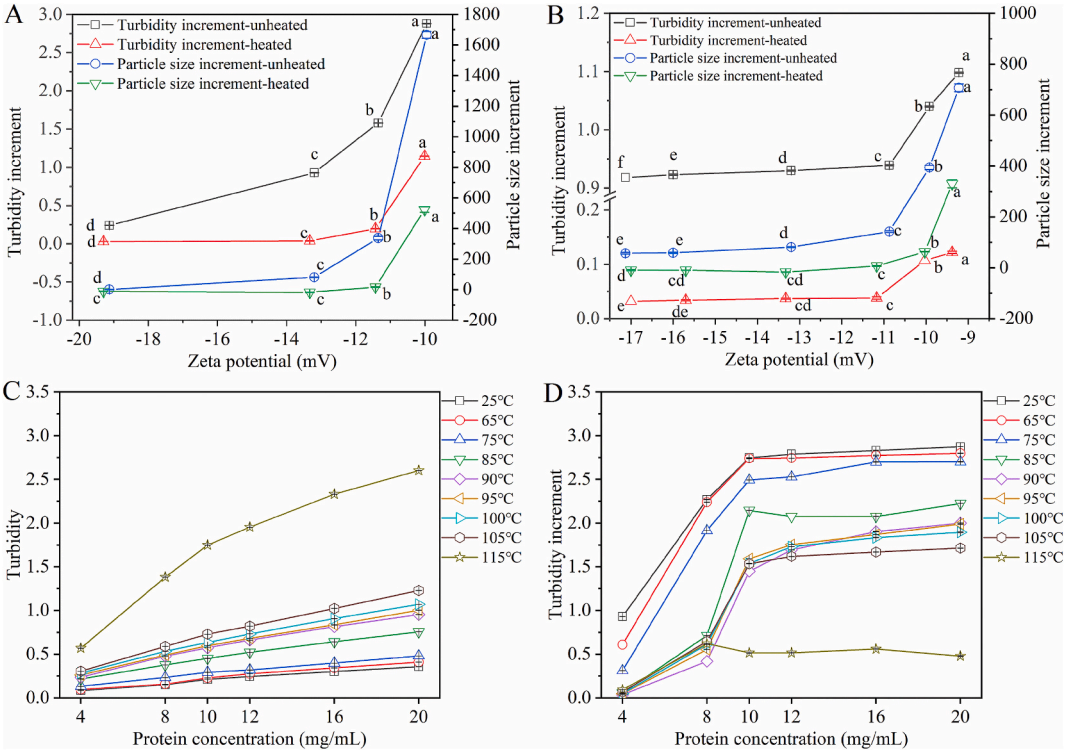

Fig. 6. Effect of zeta potential on the turbidity increment and particle size increment of Mg^{2+} coagulated unheated and 90 °C heated defatted soymilk coagulated with different Mg^{2+} concentrations (A) or by different soy protein concentrations (B). Turbidity of different temperatures heated defatted soymilk at different protein concentrations (C) and the corresponding turbidity increment (D). Different letters in the same series indicate significant differences ($P < 0.05$).

concentration and varying $MgCl_2$ concentration. The results revealed that, for both unheated and heated defatted soymilks, abrupt increases in turbidity increment and particle size increment were noticed at zeta potential value of about −11 mV. In the case of fixed $MgCl_2$ concentration and varying protein concentration (Fig. 6B), turning points were also observed at the zeta potential value of about −11 mV for both unheated and heated defatted soymilks. Yang et al. (2021) reported that the zeta potential values of fermentation-induced soy protein gels were about −10 mV. Furthermore, in either acid- or Ca^{2+} – induced coagulation of soymilk, larger aggregates were formed when zeta potential reached the value of −11 mV (Ringgenberg et al., 2013; Wang et al., 2015). Therefore, a critical zeta potential value of −11 mV was required so as to induce significant Mg^{2+} coagulation as reflected by the abrupt increases in turbidity increment and particle size increment.

Mg^{2+} coagulation of defatted soymilks was expected to display protein concentration dependence. Since zeta potential and particle size determinations of high protein concentration defatted soymilk samples were not workable, only turbidity was measured in the higher protein concentration range.

Fig. 6C shows that the turbidity of defatted soymilks per se increased monotonically with the elevation of heating temperature and protein concentration. Several studies also reported the heat induced aggregation of soy proteins and found the similar temperature and protein concentration dependences (Chen et al., 2016, 2017; Huang et al., 2024; Liu et al., 2017; Zhao et al., 2016). Fig. 6D shows the turbidity increment induced by Mg^{2+} coagulation. It can be found that, at the low protein concentration (4 mg/mL), marked turbidity increment was occurred only for unheated, 65 °C and 75 °C heated defatted soymilks, while only negligible turbidity increments were observed for the samples which had been sufficiently heated (≥85 °C). For protein concentrations higher than 4 mg/mL but lower than 8 mg/mL, Mg^{2+} coagulation induced turbidity increments also increased slightly. A turning point was noticed at the protein concentration of 8 mg/mL. For those defatted soymilks which had been heated at temperatures higher than 85 °C, the Mg^{2+} coagulation resulted in marked increases in turbidity increment. However, for defatted soymilk which had been heated at 115 °C, no Mg^{2+} coagulation induced increase in turbidity increment was observed, possibly because the proteins were over denatured.

4. Conclusion

The Mg^{2+} binding and colloidal destabilization behavior were investigated in the BSA–small molecule mixtures and defatted soymilk. ITC results showed that the Mg^{2+} binding was mostly contributed by small molecules but proteins showed negligible binding ability. Changes of zeta potentials for BSA–small molecule mixtures and defatted soymilk with the variations of unbound Mg^{2+} concentrations followed the similar way as changes of zeta potentials for BSA with the variations of added Mg^{2+} concentrations. Therefore, only the Mg^{2+} which was not bound by small molecules was effective in reducing the zeta potentials of protein colloid particles. Turbidity and particle size of defatted soymilks increased with the elevation of Mg^{2+} concentration. A critical zeta potential value of −11 mV and a critical protein concentration of 8 mg/mL were found. The amplitudes of turbidity and particle size changes increased markedly when absolute zeta potential value was lower than 11 mV and protein concentration for heated defatted soymilk was higher than 8 mg/mL, respectively. The implication of the present study on the magnesium chloride coagulation mechanism were that the "protein-Mg^{2+}-protein bridge" was hardly formed but colloidal destabilization played crucial role in tofu making.

CRediT authorship contribution statement

Qianru Li: Writing – original draft, Methodology, Conceptualization. **Yufei Hua:** Project administration, Conceptualization. **Xingfei Li:** Software, Formal analysis, Data curation. **Xiangzhen Kong:** Writing – review & editing. **Caimeng Zhang:** Visualization, Resources. **Yeming Chen:** Visualization, Resources.

Declaration of competing interest

The authors declare that they have no known competing financial interests or personal relationships that could have appeared to influence the work reported in this paper.

Acknowledgment

This work was supported by the Key Research and Development Program of Shandong Province (2022CXGC010603), the National Natural Science Foundation of China (32272243, 32072164), and the China Postdoctoral Science Foundation (2020M671342).

Data availability

Data will be made available on request.

References

Bauland, J., Famelart, M. H., Bouhallab, S., Jeantet, R., Roustel, S., Faiveley, M., & Croguennec, T. (2020). Addition of calcium and magnesium chlorides as simple means of varying bound and precipitated minerals in casein micelle: Effect on enzymatic coagulation. *Journal of Dairy Science, 103*(11), 9923–9935. https://doi.org/10.3168/jds.2020-18749

Benherlal, P. S., & Arumughan, C. (2007). Chemical composition and *in vitro* antioxidant studies on *Syzygium cumini* fruit. *Journal of the Science of Food and Agriculture, 87*(14), 2560–2569. https://doi.org/10.1002/jsfa.2957

Canabady-Rochelle, L.-S., Sanchez, C., Mellema, M., & Banon, S. (2009). Study of calcium−soy protein interactions by isothermal titration calorimetry and pH cycle. *Journal of Agricultural and Food Chemistry, 57*(13), 5939–5947. https://doi.org/10.1021/jf900424b

Chen, N., Zhao, M., Chassenieux, C., & Nicolai, T. (2016). Thermal aggregation and gelation of soy globulin at neutral pH. *Food Hydrocolloids, 61*, 740–746. https://doi.org/10.1016/j.foodhyd.2016.06.028

Chen, N., Zhao, M., Chassenieux, C., & Nicolai, T. (2017). The effect of adding NaCl on thermal aggregation and gelation of soy protein isolate. *Food Hydrocolloids, 70*, 88–95. https://doi.org/10.1016/j.foodhyd.2017.03.024

Chen, Y., Liao, X., Zhang, C., Kong, X., & Hua, Y. (2022). Hydrolyzing behaviors of endogenous proteases on proteins in sesame milk and application for producing low-phytate sesame protein hydrolysate. *Food Chemistry, 385*, Article 132617. https://doi.org/10.1016/j.foodchem.2022.132617

Gołębiowski, A., & Buszewski, B. (2023). Characterization of colloidal particles of a biological and metallic nature. *Microchemical Journal, 191*, Article 108864. https://doi.org/10.1016/j.microc.2023.108864

Guan, X., Zhong, X., Lu, Y., Du, X., Jia, R., Li, H., & Zhang, M. (2021). Changes of soybean protein during tofu processing. *Foods, 10*(7), 1594. https://doi.org/10.3390/foods10071594

Horne, D. S., & Banks, J. M. (2004). Rennet-induced coagulation of milk. In *, Vol. 1. Cheese: Chemistry, physics and microbiology* (pp. 47–70). Elsevier. https://doi.org/10.1016/S1874-558X(04)80062-9.

Huang, L., Yan, Y., Qu, L., Li, F., Chen, L., & Li, Y. (2024). Structure, emulsifying and embedding characteristics of soy protein isolate induced by the complexation of carrageenan with different charge groups. *Food Hydrocolloids, 157*, Article 110455. https://doi.org/10.1016/j.foodhyd.2024.110455

Johnson, R. A., Manley, O. M., Spuches, A. M., & Grossoehme, N. E. (2016). Dissecting ITC data of metal ions binding to ligands and proteins. *Biochimica et Biophysica Acta (BBA) - General Subjects, 1860*(5), 892–901. https://doi.org/10.1016/j.bbagen.2015.08.018

Kao, F.-J., Su, N.-W., & Lee, M.-H. (2003). Effect of calcium sulfate concentration in soymilk on the microstructure of firm tofu and the protein constitutions in tofu whey. *Journal of Agricultural and Food Chemistry, 51*(21), 6211–6216. https://doi.org/10.1021/jf0342021

Kaspchak, E., Igarashi-Mafra, L., & Mafra, M. R. (2018). Influence of ternary complexation between bovine serum albumin, sodium phytate, and divalent salts on turbidity and *in vitro* digestibility of protein. *Journal of Agricultural and Food Chemistry, 66*(40), 10543–10551. https://doi.org/10.1021/acs.jafc.8b03142

Kim, O.-H., Kim, Y.-O., Shim, J.-H., Jung, Y.-S., Jung, W.-J., Choi, W.-C., Lee, H., Lee, S.-J., Kim, K.-K., Auh, J.-H., Kim, H., Kim, J.-W., Oh, T.-K., & Oh, B.-C. (2010). β-Propeller phytase hydrolyzes insoluble Ca^{2+}-phytate salts and completely abrogates the ability of phytate to chelate metal ions. *Biochemistry, 49*(47), 10216–10227. https://doi.org/10.1021/bi1010249

Kulmyrzaev, A., Chanamai, R., & McClements, D. J. (2000). Influence of pH and $CaCl_2$ on the stability of dilute whey protein stabilized emulsions. *Food Research International, 33*(1), 15–20. https://doi.org/10.1016/S0963-9969(00)00018-1

Kumagai, H., Ishida, S., Koizumi, A., Sakurai, H., & Kumagai, H. (2002). Preparation of phytate-removed deamidated soybean globulins by ion exchangers and

characterization of their calcium-binding ability. *Journal of Agricultural and Food Chemistry, 50*(1), 172–176. https://doi.org/10.1021/jf011011u

Kunde, S. S., & Wairkar, S. (2022). Targeted delivery of albumin nanoparticles for breast cancer: A review. *Colloids and Surfaces B: Biointerfaces, 213*, Article 112422. https://doi.org/10.1016/j.colsurfb.2022.112422

Lee, C. H., & Rha, C. (1978). Microstructure of soybean protein aggregates and its relation to the physical and textural properties of the curd. *Journal of Food Science, 43*(1), 79–84. https://doi.org/10.1111/j.1365-2621.1978.tb09740.x

Liang, G., Chen, W., Qie, X., Zeng, M., Qin, F., He, Z., & Chen, J. (2020). Modification of soy protein isolates using combined pre-heat treatment and controlled enzymatic hydrolysis for improving foaming properties. *Food Hydrocolloids, 105*, Article 105764. https://doi.org/10.1016/j.foodhyd.2020.105764

Liu, J., Shim, Y. Y., Shen, J., Wang, Y., & Reaney, M. J. T. (2017). Whey protein isolate and flaxseed (*Linum usitatissimum* L.) gum electrostatic coacervates: Turbidity and rheology. *Food Hydrocolloids, 64*, 18–27. https://doi.org/10.1016/j.foodhyd.2016.10.006

Liu, Y., Lu, S., Meng, J., Xiang, H., Korma, S. A., Cacciotti, I., & Cui, C. (2023). Complexation between egg yolk protein hydrolysate, phytic acid and calcium ion: Binding mechanisms and influence on protein digestibility and calcium uptake. *LWT, 184*, Article 114986. https://doi.org/10.1016/j.lwt.2023.114986

Madjirebaye, P., Peng, F., Huang, T., Liu, Z., Mueed, A., Pahane, M. M., … Peng, Z. (2022). Effects of fermentation conditions on bioactive substances in lactic acid bacteria-fermented soymilk and its storage stability assessment. *Food Bioscience, 50*, Article 102207. https://doi.org/10.1016/j.fbio.2022.102207

Narong, P., & James, A. E. (2006). Effect of pH on the ζ-potential and turbidity of yeast suspensions. *Colloids and Surfaces A: Physicochemical and Engineering Aspects, 274*(1–3), 130–137. https://doi.org/10.1016/j.colsurfa.2005.08.042

Oh, D. J., Han, M. S., & Ahn, K. H. (2007). Metal-containing trifurcate chemosensing ensemble for phytate. *Supramolecular Chemistry, 19*(4–5), 315–320. https://doi.org/10.1080/10610270701355034

Patra, T., Rinnan, Å., & Olsen, K. (2021). The physical stability of plant-based drinks and the analysis methods thereof. *Food Hydrocolloids, 118*, Article 106770. https://doi.org/10.1016/j.foodhyd.2021.106770

Philippe, M., Le Graët, Y., & Gaucheron, F. (2005). The effects of different cations on the physicochemical characteristics of casein micelles. *Food Chemistry, 90*(4), 673–683. https://doi.org/10.1016/j.foodchem.2004.06.001

Rao, A. G., & Rao, M. S. (1975). Binding of mg (II) by the 11S fraction of soybean proteins. *Journal of Agricultural and Food Chemistry, 23*(4), 657–661. https://doi.org/10.1021/jf60200a001

Ringgenberg, E., Alexander, M., & Corredig, M. (2013). Effect of concentration and incubation temperature on the acid induced aggregation of soymilk. *Food Hydrocolloids, 30*(1), 463–469. https://doi.org/10.1016/j.foodhyd.2012.05.011

Saio, K., Koyama, E., & Watanabe, T. (1967). Protein-calcium-phytic acid relationships in soybean: Part I. Effects of calcium and phosphorus on solubility characteristics of soybean meal protein. *Agricultural and Biological Chemistry, 31*(10), 1195–1200. https://doi.org/10.1080/00021369.1967.10858947

Sakakibara, M., & Noguchi, H. (1977). Interaction of 11S fraction of soybean protein with calcium ion. *Agricultural and Biological Chemistry, 41*(9), 1575–1580. https://doi.org/10.1080/00021369.1977.10862744

Saponaro, A. (2018). Isothermal titration calorimetry: A biophysical method to characterize the interaction between label-free biomolecules in solution. *Bio-Protocol, 8*(15), Article e2957. https://doi.org/10.21769/BioProtoc.2957

Serrano-Lotina, A., Portela, R., Baeza, P., Alcolea-Rodriguez, V., Villarroel, M., & Ávila, P. (2023). Zeta potential as a tool for functional materials development. *Catalysis Today, 423*, Article 113862. https://doi.org/10.1016/j.cattod.2022.08.004

Wang, B., Wang, Q., Wang, B., Wang, S., Zhang, Y., & Zhao, D. (2023). From soybeans to tofu: The underlying chemistry. *Journal of Chemical Education, 100*(9), 3724–3730. https://doi.org/10.1021/acs.jchemed.3c00096

Wang, R., Xie, L., & Guo, S. (2015). Effects of small molecular compounds in soymilk on the protein coagulation process: Ca^{2+} as coagulant. *Food Research International, 77*, 34–42. https://doi.org/10.1016/j.foodres.2015.04.019

Wang, W., Tan, K. W. J., Chiang, P. L., Wong, W. X., Chen, W., & Lin, Q. (2023). Impact of incorporating free calcium and magnesium on the heat stability of a dairy- and soy-protein-containing model emulsion. *Polymers, 15*(22), 4424. https://doi.org/10.3390/polym15224424

Yang, X., Ke, C., & Li, L. (2021). Physicochemical, rheological and digestive characteristics of soy protein isolate gel induced by lactic acid bacteria. *Journal of Food Engineering, 292*, Article 110243. https://doi.org/10.1016/j.jfoodeng.2020.110243

Yıldız, A., Kara, A. A., & Acartürk, F. (2020). Peptide-protein based nanofibers in pharmaceutical and biomedical applications. *International Journal of Biological Macromolecules, 148*, 1084–1097. https://doi.org/10.1016/j.ijbiomac.2019.12.275

Zhao, H., Li, W., Qin, F., & Chen, J. (2016). Calcium sulphate-induced soya bean protein tofu-type gels: Influence of denaturation and particle size. *International Journal of Food Science & Technology, 51*(3), 731–741. https://doi.org/10.1111/ijfs.13010

Zhao, X., Wang, C., Cheng, M., Zhang, X., & Jiang, H. (2021). Influence of calcium on the properties of micellar casein in goat milk. *LWT, 150*, Article 111935. https://doi.org/10.1016/j.lwt.2021.111935

Zheng, Y., Li, L., Jin, Z., An, P., Yang, S.-T., Fei, Y., & Liu, G. (2021). Characterization of fermented soymilk by Schleiferilactobacillus harbinensis M1, based on the whole-genome sequence and corresponding phenotypes. *LWT, 144*, Article 111237. https://doi.org/10.1016/j.lwt.2021.111237